Geophysica (1996), 32(1-2), 7-34

Long Paleoclimate Records from China

N.W. Rutter[1], Zhongli Ding[2], Tungsheng Liu[2]

[1]Department of Earth and Atmospheric Sciences, University of Alberta, Edmonton, Canada T6E 2E3
[2]Institute of Geology, Chinese Academy of Science P.O. Box 634, Beijing, China

(Received: December 1995; Accepted: June 1996)

Abstract

The loess-paleosol sequences in the Loess Plateau of north-central China offer some of the most complete Quaternary terrestrial deposits anywhere. The Baoji section consists of 37 field identified paleosols formed during the last 2.5 Ma. B horizons vary from Bw to very strong Bt's and were developed under forest and/or steppe-forest environments. The loess is derived from the west and northwest and carried by northwest winds into the Plateau area. It is accepted that during glacial times wind velocity was stronger resulting in higher loess accumulation and larger average grain size than during interglacial times when soils developed where there was less accumulation and finer average grain size. A grain size time scale was constructed from the Baoji section back to 2.5 Ma based on orbital variations, independent of the deep sea $\delta^{18}O$ isotope records. There is close climatic correlation between the Baoji grain size time scale and DSDP site 607 $\delta^{18}O$ records from the North Atlantic for the last 1.67 Ma. In the northwest part of the Loess Plateau we obtained high resolution magnetic susceptibility and grain size data from the Lijia Yuan section that enabled us to differentiate between several soil and loess units of the last glacial-interglacial cycle. These data were correlatable with SPECMAP $\delta^{18}O$ isotope and GISP2 $\delta^{18}O$ ice core data. Thus, our climatic proxy records, compared with other records, have enabled us to make inferences on both regional and global climatic patterns. These include the influence of the uplift of the Tibetan Plateau on the worldwide change of climate at about 2.5 Ma, the link between the variations of the East Asian winter monsoon and global ice volume, and that our high resolution records can record regional, and perhaps global, rapid, short term (millennial scale) climatic oscillations.

Key words: loess, paleosol, Quaternary, orbital variation, grain size, magnetic susceptibility.

1. Introduction

Over the past eight years, we have been investigating the loess-paleosol sequences of north-central China in view of reconstructing past climates and environments, and determining climate forcing mechanisms. We have concentrated mainly on the Baoji section, one of the most complete sequences in the Loess Plateau, representing an almost continuous depositional record for about the past 2.5 Ma (*Rutter et al.*, 1991). The purpose of this paper is to review significant research results as well as to compare our data with data from other Quaternary records, specifically ice-core and deep sea records, and to elucidate on forcing mechanisms and linkages between various climate elements.

Loess-paleosol sequences representing nearly continuous records, similar to the Baoji section, are found in several areas (*Liu et al.*, 1985). Loess was shifted from inland deserts of northwestern China under cold, dry and windy environments prominent during glacial periods, whereas soils developed under relatively warm and wet climates during interglacial times. The alternation of loess-paleosol units is triggered by a change in insolation induced by variations in the earth's orbit, but effected by interactions of a number of local physical factors, such as the Asian monsoon. Therefore, the study of these sequences gives us a unique opportunity to describe and understand climates on a local and on a global scale.

2. *The Baoji section*

The Baoji section is located about 5 km north of the city of Baoji, in the southern-most part of the Loess Plateau (*Rutter et al.*, 1991, Fig. 1). It is exposed below the

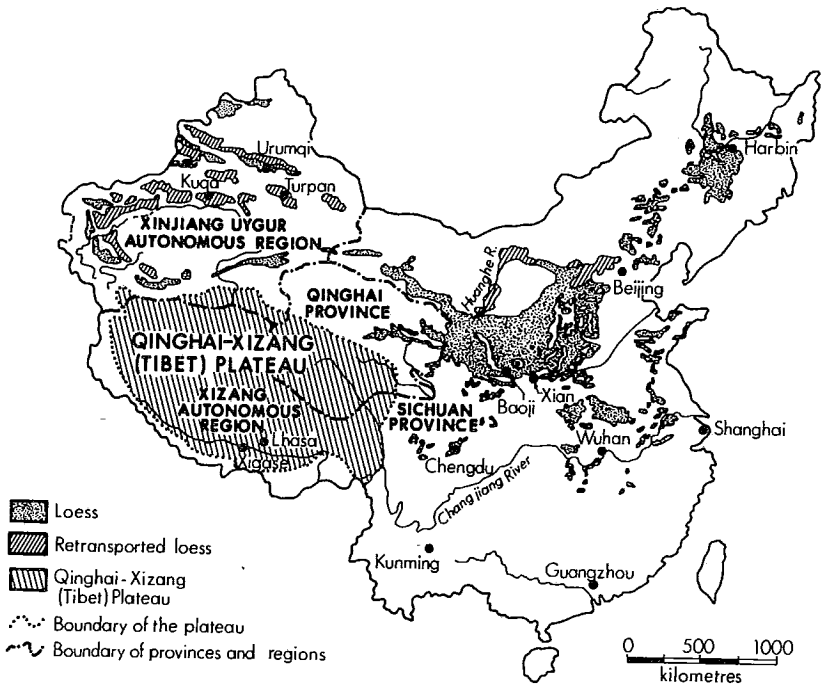

Fig. 1. Map of China showing loess areas and the Tibetan Plateau. The Baoji section is located at the southern most part of the Loess Plateau.

"Yuan", a broad, flat, high table land at an elevation of about 970 m above sea level (34°20′N, 107°00′E). The thickness of loess is about 160 m underlain by the Red Clay Formation. Traditionally, the loess sequence in China has been divided into three formations - the Malan, Lishi and Wucheng. The lower Wucheng Loess is separated from the overlying Lishi Loess by stratigraphic marker L15, a unit of thick coarse silt

readily recognizable in the field. Lishi Loess is overlain by Malan Loess, L1, which accumulated during the last glacial and supports the Holocene soil, S0.

The section consists of thirty-seven clearly defined paleosols (Fig. 2), including multiple paleosol units S2, S5 and S9. Based on macro and micromorphological observations, the major pedogenic processes involved in the formation of the Baoji

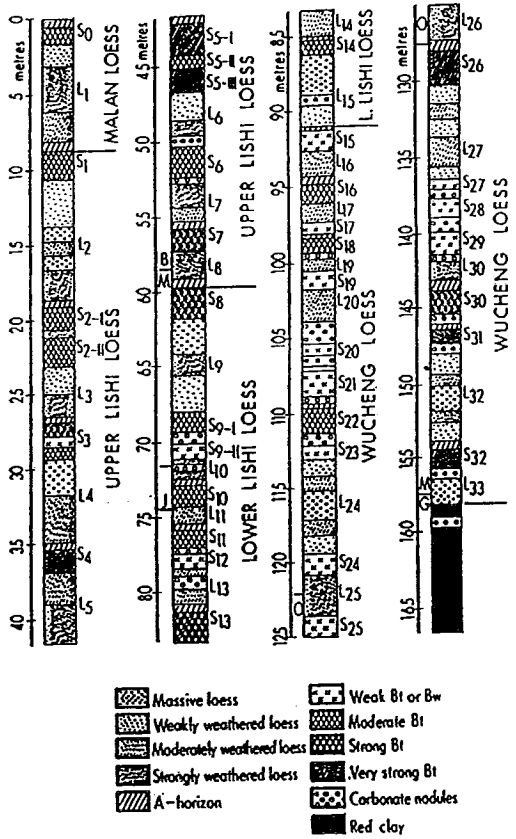

Fig. 2. Loess-paleosol sequence at Baoji with designation of the major soil horizons. Paleomagnetic reversals are indicated - B = Brunhes, M = Matuyama, J = Jaramillo, O = Olduvai, G = Gauss.

paleosols are believed to be carbonate eluviation and illuviation, clay translocation, pseudogleyization and rubification (*Rutter* and *Ding,* 1993). The diagnostic B horizons of the 37 soils are classified into four types - Bw, or weak Bt, moderate B, strong Bt and very strong Bt. The Holocene soil at Baoji contains a moderately developed Bt, which was formed under steppe-forest vegetation. Most of the soils with Bt horizons comparable to the Holocene soil are interpreted as developed under forest and/or steppe-forest environments. Two extremely warm and humid periods are represented by the exceptionally well-developed soils of S5 and S26. These events occurred at about 0.55 Ma and 1.8 Ma respectively.

Most loess beds have been leached of primary carbonates resulting in loess beds acquiring weak to strong granular structures. The loess is subdivided into four types - massive, weakly weathered, moderately weathered and strongly weathered. They are believed to have accumulated under steppe environments (*Rutter* and *Ding,* 1993). Exceptionally cold, dry, and windy periods are represented by relatively coarse grained and thick loess beds L2, L9, L15, L24, L27 and L32 (Fig. 2). This occurred at about 0.16, 0.85, 1.2, 1.6, 2.0 and 2.4 Ma respectively.

Geochronological control of the Baoji paleosols initially were based on magnetostratigraphy with the Brunhes, Matuyama and Gauss chrons, and Jaramillo and Olduvai events clearly recognized (*Rutter et al.,* 1990). Later, minimum-age estimates of each loess unit were calculated by linear interpolation between magnetic time controls (*Rutter et al.,* 1991) and a recently constructed orbital timescale (*Ding et al.,* 1994). The Baoji paleosols can be correlated with equivalent pedostratigraphic units throughout the Loess Plateau by a combination of magnetostratigraphy, magnetic susceptibility, and the character, position, and association of the pedostratigraphic units within the Quaternary succession.

The oscillations between primary soil development and loess deposition during the past 2.5 Ma have provided evidence for the variations between timing, duration and intensity of southeast and southwest migration of the winter monsoon and the northwest migration of the summer monsoon (Fig. 3, *Rutter* and *Ding,* 1993). Using the ages of

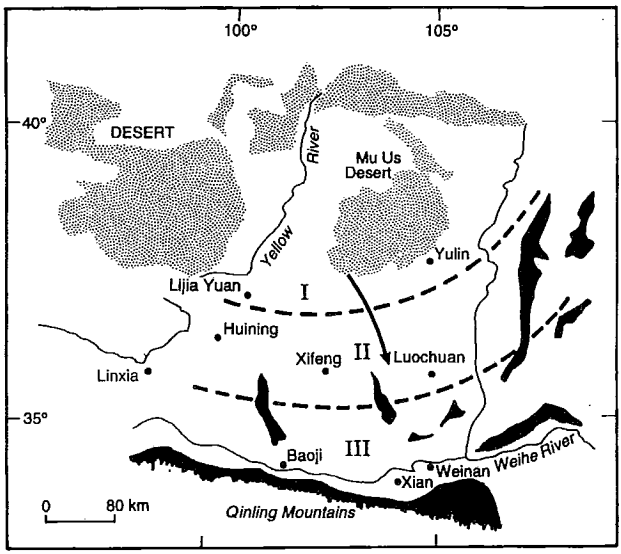

Fig. 3. Schematic map showing the zonation of loess in the Loess Plateau: zone I-sandy loess, zone II-loess and zone III-clayey loess. Grain size and thickness of loess deposits display a continuous decrease from zone I to zone III. The arrow indicates the dominant subaerial wind direction in winter seasons, coinciding with the decrease in grain size and thickness of the loess. The deserts (dotted) and mountains (black) around and within the Loess Plateau are indicated (modified from *Liu et al.*, 1985).

magnetic reversals and interpolation of estimated sedimentation rates, the Baoji record was then compared to the marine isotope record (*Rutter et al.*, 1991). It is clearly shown in Figure 4, that orbital variations affecting solar insolation are reflected in the timing of soil development and loess deposition. The 100 ka eccentricity cycle dominates in the last 0.6 to 0.8 Ma, the 41 ka obliquity signal is prominent to about 1.6 Ma to 0.6 - 0.8 Ma, while below 1.6 Ma a mixed pattern is recorded.

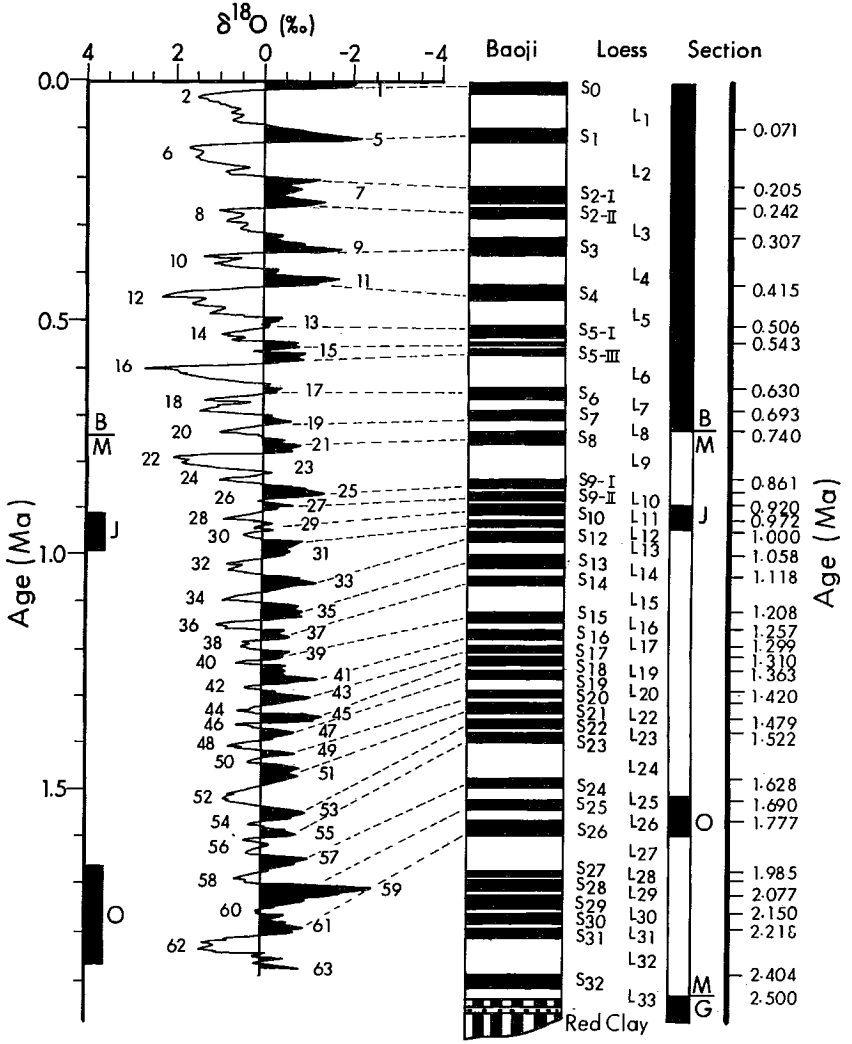

Fig. 4 . Left: Composite record of four individual normalized oxygen isotope records plotted against time (*Williams et al.*, 1988). Right: The Baoji type pedostratigraphic section showing the relative thickness of paleosol (black) and loess (white) units. The paleomagnetic chrons and subchrons for the Baoji section are plotted to aid in correlation (B = Brunhes, M = Matuyama, J = Jaramillo, O = Olduvai, G = Gauss). Minimum-age estimates of each loess unti have been calculated by linear interpretation between magnetic time controls.

3. *Magnetic susceptibility record*

Magnetic susceptibility has been utilized to detect paleoclimatic variations and in correlating paleosols throughout the Loess Plateau. It has been useful in detecting gross climatic variations through time, and in some cases, in detecting climatic change at higher resolution than field identifiable paleosols. The first studies on magnetic susceptibility in China were by *Heller* and *Liu* in 1984, and later by such workers as *Kukla et al.* (1988) in sections such as Luochuan and Xifeng. In the Baoji section magnetic susceptibility shows that during cold periods when loess deposition is high the relative susceptibility is low, whereas during warmer periods when deposition of loess is lower, and soils develop, the susceptibility signal is higher. This is opposite to some areas outside of China, like the Kurtak section in the Altai Mountain area of south-central Siberia (*Rutter et al.*, 1995). Figure 5 shows the susceptibility curve of the Baoji section, where about 1600 readings at 10 cm spacing were taken. The signals separate the loess units and soils similar to what can be identified in the field. Although gross correlation between sections in the Loess Plateau is good, in detail, minor climatic fluctuations are not always correlatable on a regional scale. There are exceptions such as the Xifeng and Luochuan sections correlated by *Kukla et al.* (1988). It may be that they show similar characteristics because the sections are relatively close together

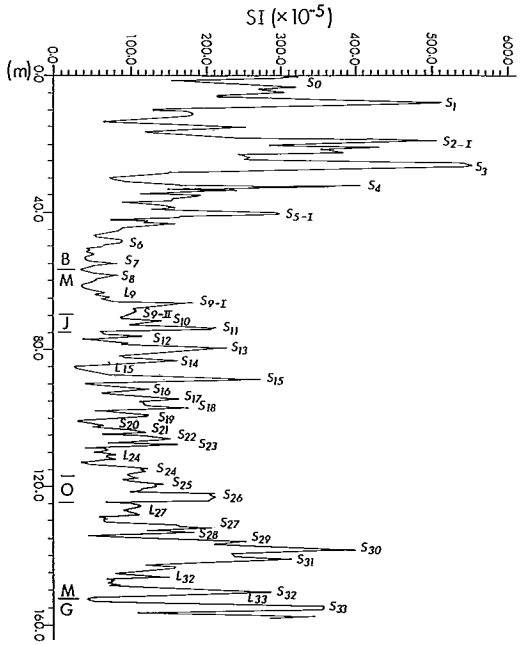

Fig. 5. Magnetic susceptibility of the Baoji section. Susceptibility was measured at 10 cm intervals using a Bartington MSII susceptibility meter.

and they have been subjected to a similar climatic and depositional history. However, correlating the Xifeng section with our Yulin section, located near the northern border of the Loess Plateau and about 500 km away from the Xifeng section, only major climatic variations can be correlated. This may be due to depositional rate variations, local hiatuses and sample spacing differences. A larger problem however, is our lack of understanding on the origin of magnetic susceptibility. There are several theories such as the enrichment of detrital magnetic minerals in soils during interglacials (*Heller* and *Liu,* 1984), sub-aerial deposition from high level transport of ultra-fine magnetic particles (*Kukla et al.,* 1988; *Kukla* and *An,* 1989) and in situ authigenesis of magnetite during soil forming processes (*Maher* and *Thompson,* 1991). No matter what the origin, susceptibility signals have been useful in correlating soil units and identifying orbital periodicities (*Liu et al.,* 1992).

4. Grain size

One of the most significant discoveries during our investigations is the importance of loess grain size as a paleoclimate proxy (*Rutter,* 1992; *Ding et al.,* 1993; 1994). This assumes that the grain size of a representative sample is a reflection of wind velocity and that the source and wind directions are relatively constant. It is widely accepted that the source of loess is from the west and northwest of the Loess Plateau, that the dominant winter monsoonal wind is from the northwest, and that the wind direction was relatively constant throughout the Quaternary (Fig. 3). Further, it is accepted that in this region, wind velocity was higher during glacial times (cooler), than during interglacials (warmer). This set of conditions results in a greater accumulation rate and a size increase during glacials and a lower accumulation rate and overall smaller grain size during interglacials. The slower accumulation rate and warmer climate provides the necessary environment for soils to form. Also, there is an overall decrease in modal size from northwest to southeast, coinciding with the southeastward decrease in thickness of loess units (*Liu et al.,* 1966; Fig. 3). The cause of variation in wind velocity is related to the East Asia winter monsoon, itself a dynamic interaction of the Earth's ocean-continent-atmosphere (Fig. 6). The winter monsoon shows extensive variability on time scales from annual cycles to glacial-interglacial rhythms (*An et al.,* 1991). The annual cycle of solar radiation leads to increased cooling of the middle-latitude land surface over eastern Asia during the northern hemisphere winter season, compared to the surrounding oceans which have a much higher heat capacity than the land surface. The strong winter cooling of the atmosphere over land causes a descending motion and the development of a high-pressure cell over Siberia and Mongolia (referred to as the Siberian High). Coupling of the Siberia High with the Aleutian Low over the northwestern Pacific Ocean results in a vigorous cold-dry air outflow from land to ocean. In north-central China, this winter monsoon exerts a strong control on the climate from September to May with dominant winds from a

northwesterly direction. This is consistent with the decrease in mean grain size of the loess from northwest to southeast (Fig. 3).

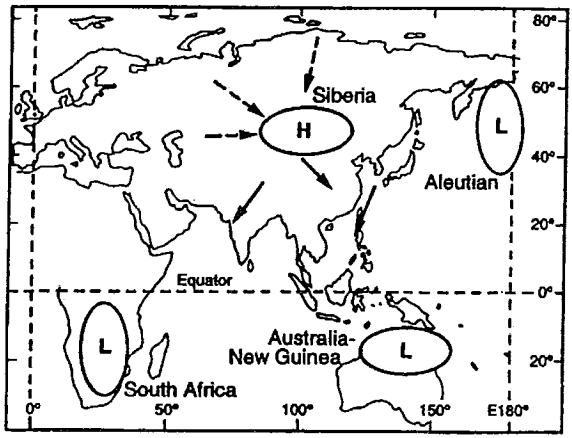

Fig. 6. Schematic map showing the positions of the high and low pressure cells controlling the East-Asian winter monsoon circulation. The solid arrows indicate the directions of the northwesterly and northeasterly monsoonal winds and the dashed arrows show the pathways of the polar cold air reaching the Siberian region and accumulating there to develop and strengthen the Siberia High (modified from *Tao* and *Chen*, 1957).

Particle size measurements of some typical loess-soil samples taken in different localities on the Plateau show that the grains are concentrated almost completely in the fractions below 50 μm. The fraction ranging from 50 to 10 μm, and smaller than 2 μm show the most variability, with the variability within the fraction between 10 and 2 μm being minor. The measurements also suggest that pedogenic weathering can only make a limited or negligible contribution to the grain size distribution of loess deposits (*Ding et al.*, 1994). The ratio of the fraction smaller than 2 μm (%) to the fraction greater than 10 μm (%) is used as a grain size index. Results show that this grain size index is very sensitive to loess-soil alternations (*Ding et al.*, 1994; Fig. 7). The grain size profile is then employed to represent the glacial-interglacial cyclic variation in the intensity of the East Asia winter monsoon and as a proxy indicator of winter monsoon circulation.

We have tuned our Baoji grain size record to the orbital time scale (*Ding et al.*, 1994) with the approach developed by *Imbrie et al.*, (1984). The tuning is independent of any correlation with $\delta^{18}O$ signals from deep sea sediments. First, we used the ETP curve formulated from theoretical changes of the three orbital elements recently calculated by *Berger and Loutre* (1991) as the tuning target. The same time lags are used for grain size as the SPECMAP $\delta^{18}O$ stack, being 8000 years for the obliquity and 5000 years for the reversed precession signals. We used the Brunhes/Matuyama boundary (730,000 years BP) located within the loess unit L8 and the stacked SPECMAP $\delta^{18}O$ events 2.0 (12,000 yr), 5.0 (71,000 yr) and 6.0 (128,000 yr) as initial time controls. Previous studies (*Liu et al.*, 1985; *Kukla*, 1987; *Kukla* and *An*, 1989)

have revealed that the isotopic event 2.0 can be correlated to the top of L1, and the events 5.0 and 6.0 to the top and bottom of S1 in the Chinese loess stratigraphy (Fig. 4). We developed an initial time scale using linear interpolation between the initial time controls, assuming that the loess deposition rate during glacial periods is twice that during interglacial times. Finally, we repeatedly applied digital filters to extract the frequency components with central periods of 41,000 and 21,000 years from the grain size data plotted against the initial time scale, and aligned the filtered curves against the corresponding phase-locked obliquity and precession signals by adding new time control points (*Ding et al.,* 1994). Figure 8 shows the final version of the orbitally-tuned time scale over the past 2.5 Ma years. The filtered frequency components correlate well with the theoretical variations of the obliquity and precession data, whereas above about 0.55 Ma the filtered eccentricity signals began to match the theoretical cycles with an increase in amplitude. The Baoji grain size time scale has been examined by several approaches using different criteria (*Ding et al.,* 1994). Favorable comparisons with dated magnetic reversals, cross-spectral analysis and tuned $\delta^{18}O$ records attest to the reasonable nature of the time scale.

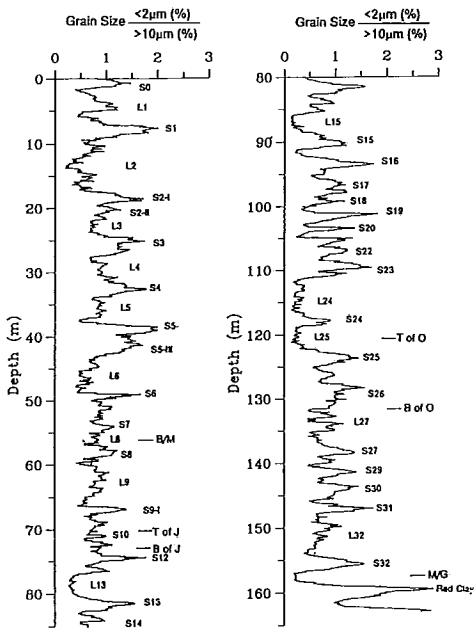

Fig. 7. Grain size variation of the Baoji loess-soil section, plotted on a depth scale with the numbering of the loess (L) and soil (S) units. Grain size index expressed in the ratio of the fraction smaller than 2 μm (%) to that larger than 10 μm (%). Major magnetic reversals (Brunhes/Matuyama boundary, Jaramillo and Olduvai subchrons, and Matuyama/Gauss boundary) tied to the loess-soil sequence are shown.

Recently, *Shackleton et al.* (1990), in tuning the ODP 677 astronomical time scale, have inferred an 'extra' obliquity cycle in the lower Brunhes, and extended the age of the B/M boundary to about 0.78 Ma. This time scale has since been supported by a wide range of convincing evidence, including the re-analysis of radiometric dates of this magnetic reversal (*Baksi et al.*, 1992; *Tauxe et al.*, 1992). In this case, the SPECMAP time scale needs to be refined beyond 0.62 Ma. Our Baoji time scale yields an age of about 0.75 Ma for the B/M boundary, showing substantial difference with both the SPECMAP and ODP 677 time scales. Another puzzling feature is that the B/M magnetic reversal is registered in the lower part of stage 19 in the SPECMAP record, whereas it is defined in the middle of L8, a counterpart of isotope stage 20. The difference of depositional age between the two records may be up to 10,000 years, if we don't take the magnetic lock-in depth into consideration. At any rate, it should be kept in mind that due to the 'B/M boundary problem', the reliability of both the SPECMAP and grain size time series may be somewhat problematic over the 0.62 - 0.78 Ma interval.

Spectral analysis of the grain size record clearly shows time dependent monsoonal periodicities (Fig. 9). In the past 0.6 Ma, the strongest power is centered at about the 100 ka eccentricity period with a lesser peak at 41 ka, and still lesser at the 23 and 19 ka precessional peaks. Over the time interval 0.8 - 1.6 Ma, the 41 ka obliquity power becomes dominant whereas the 100 ka eccentricity-associated periodicity is not detected. Between 0.55 Ma and 1.0 Ma both the 100 ka and 41 ka periods are very strong. The climatic periodicities are rather complex over the interval from 1.6 to 2.5 Ma. There are seven well constrained peaks in the spectrum, centered near the 19 ka, 23 ka, 29 ka, 41 ka, 55 ka, 90 ka, and 400 ka periodicities. The 400 ka and 55 ka periodicities are the strongest, whereas the 90 ka, 41 ka, 29 ka, 23 ka and 19 ka are not as strong. Therefore, these spectral analyses suggest that there are at least two shifts of dominant periodicities in the long-term monsoon variation. The first shift occurred around 1.6 Ma, and is characterized by the change in power concentrations from low frequency cycles to 41 ka obliquity oscillations. The timing of the second shift, from 41 ka to 100 ka cycles take place at roughly 0.6 ka.

5. *Comparison with other long records*

Before we can correlate the Baoji grain size record with other long records, we must be sure that the Baoji record can be correlated to other grain size records within the region. We sampled the Weinan section about 200 km east of Baoji in 10 cm vertical intervals and analyzed and tuned the record in a similar manner to the Baoji section (Fig. 10).

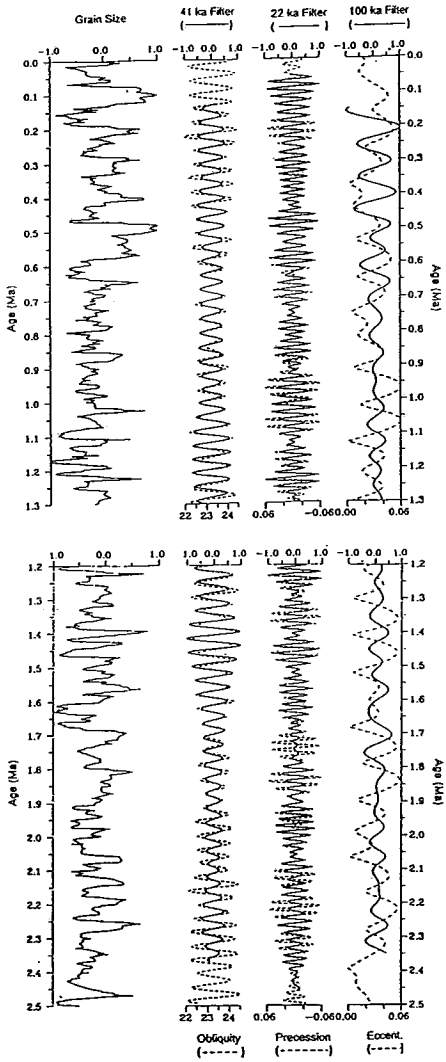

Fig. 8. Baoji grain size data plotted on BJGS time scale for the past 2.5 Ma: (left to right) normalized grain size data, filtered obliquity signal from the grain size data with a central period of 41 ka (solid line) versus lagged orbital obliquity (dashed lines), filtered precessional signal with a central period of 22 ka (solid line) versus lagged and inverted orbital precision, and filtered eccentricity signal with a central period of 100 ka (solid line) versus orbital eccentricity (dashed line). The filtered signals are normalized.

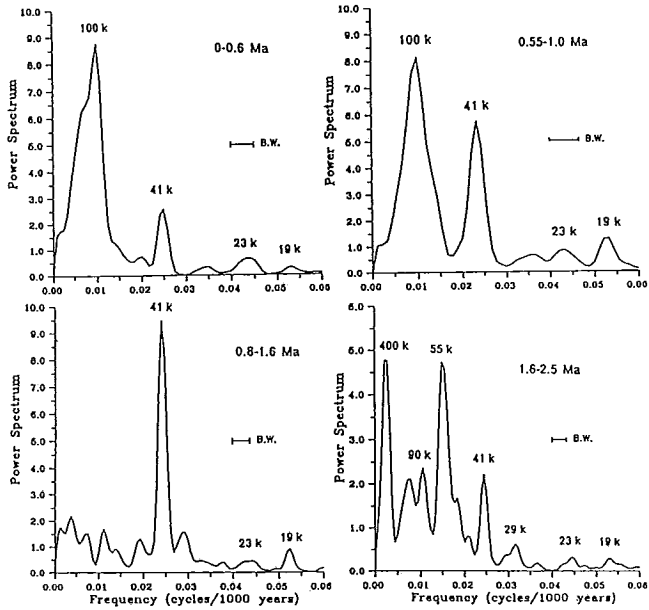

Fig. 9. Spectra of the Baoji grain size record derived from BJGS time scale over four different time intervals.

It is evident from Fig. 10 that the grain size records from Baoji and Weinan show similar trends. Most of the prominent peaks (first order and some second order) representing the 32 major soil units, identified originally by field observations, indicate warm or interglacial periods. Most second order peaks indicate other warm periods, perhaps interstadials, and can also be correlated in most cases between the two sections. However, peaks with less amplitude (third order) and relatively high frequency cannot be convincingly correlated,

From the present to about 0.8 Ma years, the correlation between soils in each section is very good, showing the same trend in grain size reduction. Thicknesses of loess units between the two sections vary somewhat, with the total thickness about 10 m thicker in the upper part of the Weinan section. Once the major soils are identified, second order peaks can be correlated with a relatively high degree of accuracy in loess units L1, L3, L4 and L6, but not in L2 and L5. Unless they are in association with a first order or second order major peak, third order peaks are difficult to correlate or to differentiate.

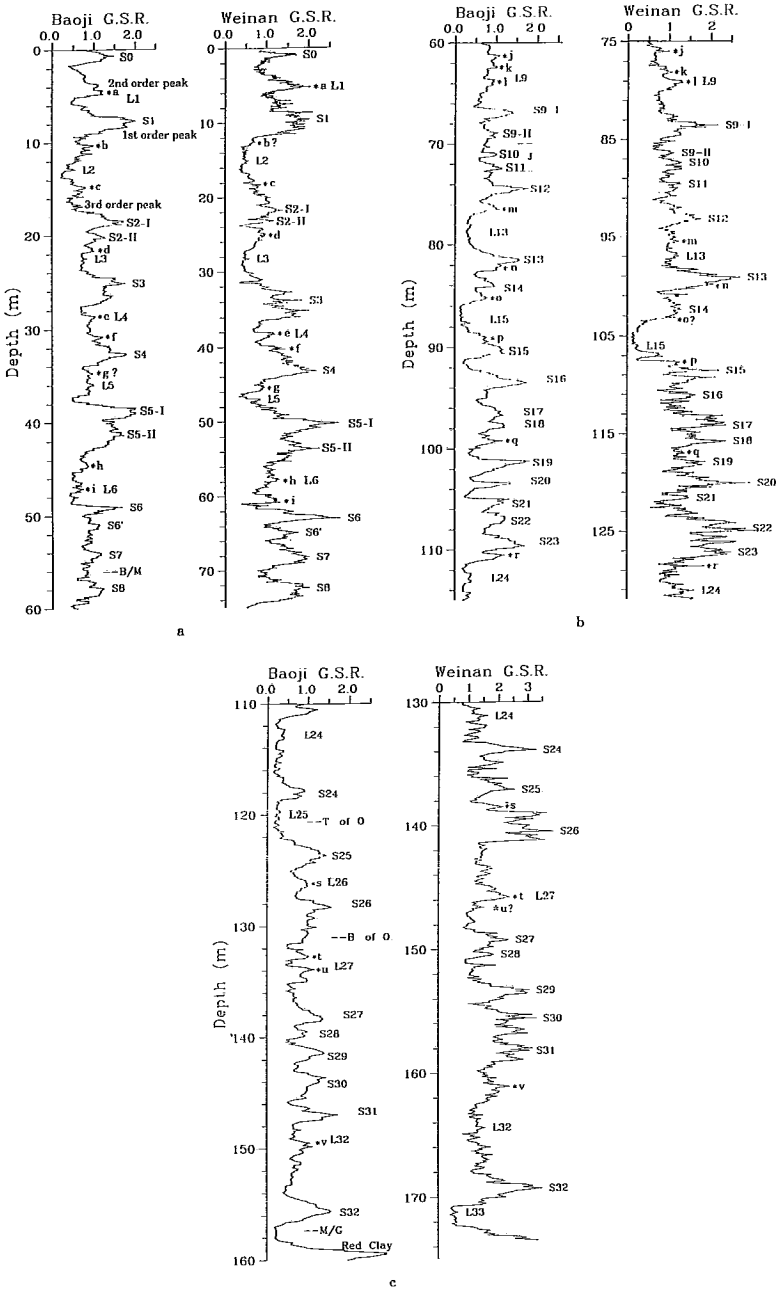

Fig. 10a,b,c. Grain size ratios of the < 2 μm (%) to the < 10 μm (%) of the Baoji and Weinan sections plotted according to depth. High ratios indicate dominance of finer grains in a soil profile, low ratios indicate loess. Soils = S0, loess units = L1, *a = other correlative peaks of the Baoji and Weinan sections. NOTE: There is a 1.5 m section missing at the lower part of the Weinan G.S.R. on Figure 10b. However, this does not alter the correlation of 1st and 2nd order peaks.

From about 0.8 Ma to 1.6 Ma, the grain size peaks representing S9-I, S12 and S13 correlate very well whereas S9-II - S11, S14 to S23 are more difficult to identify because of variations in amplitudes. This is especially true in the Weinan section because of the interference of high frequency peaks at about the same amplitude (Fig. 10). Correlation of these more difficult units is confirmed by matching the pattern of peaks within a segment of each section coupled with a knowledge of the soil characteristics and/or susceptibility signals. The second order peaks can be correlated in L9 with little trouble, whereas other second order peaks in L13-L15 and L19 are difficult to correlate because of the higher density of peaks of similar amplitudes in the Weinan section and to a lesser degree the variation of equivalent loess unit thicknesses. Finally, other peaks, both second and third order cannot be correlated with any assurance.

From 1.6 Ma to 2.5 Ma, correlation of the major soils is more difficult than those discussed above mainly because of the greater variability in thicknesses of equivalent loess units between Baoji and Weinan (Fig. 10). This is especially true in L24 and L25, where the added problems of amplitude variation between equivalent soils, greater density of peaks in the Weinan section, and peaks that are of similar amplitude as major soils but that are not major soils are evident. However, using supporting data and considering peak patterns within section segments, reliable correlation can be made. Second order peaks in L26, L27 and L32 can be matched with reasonable accuracy relying on similar patterns between the two major soils. Other peaks, both second and third order, are once again difficult to correlate or may not have corresponding units in both sections.

All in all, grain size variation at resolutions of a few thousand years can be correlated between the Baoji and Weinan sections. Although other criteria are sometimes required, the major soils representing warm phases (interglacial) and relatively high grain size ratios, as well as other less severe warming and cooling trends (interstadials) can be correlated. High resolution, third order peaks give the most difficulty.

Having established that the same grain size trends are apparent in both the Weinan and Baoji sections, we can then confidently compare the Baoji time series with the deep sea core records. Two long-term $\delta^{18}O$ records tuned to orbital time scales have recently been constructed. They are the DSDP site 607 $\delta^{18}O$ curve of the northern Atlantic (*Ruddiman et al.*, 1989a; *Raymo et al.*, 1989) and the ODP site 677 $\delta^{18}O$ record in the equatorial Pacific (*Shackleton et al.*, 1990). Both of the records have been tuned to the SPECMAP time scale (*Imbrie et al.*, 1984) for the interval above about 0.62 Ma. Below this point, *Ruddiman et al.* (1989a) and *Raymo et al.* (1989) used the (T + 1/2P) curve as a tuning target to develop the site 607 $\delta^{18}O$ time scale whereas the model output described by *Imbrie* and *Imbrie* (1980) was used in tuning the ODP 677 $\delta^{18}O$ record (*Shackleton et al.*, 1990). As some climatic events evident in the two $\delta^{18}O$

records have been related to different forcing function, ages of the magnetic reversals dated by the two records show substantial differences.

Here we compare our grain size time scale with DSDP site 607. Figure 11a shows the climatic correlation between the Baoji grain size and DSDP site 607 $\delta^{18}O$ records from the North Atlantic for the last 1.67 Ma (above the top of the Olduvai magnetic event). The grain size record is presented using a ratio of the fractions finer than 2 μm to that coarser than 10 μm so that high values represent the intervals of reduced strength of the East Asian winter monsoonal winds (*Ding et al.,* 1994). DSDP site 607 $\delta^{18}O$ is probably the most complete record of global ice volume changes in the Pleistocene (*Ruddiman et al.,* 1989a). As seen in Figure 11a, the winter monsoon record shows a close match with the global ice volume record over this time interval, with the enhanced winter monsoon periods correlating with those of extended ice sheets. At around 0.8 Ma BP there is a transitional shift from older high frequency-small amplitude changes to low frequency-large amplitude variations which is shown in both records. At around 0.6 Ma BP the long wave cycle stabilized with greatly increased amplitudes.

From the top of the Olduvai (1.67 Ma) down to the loess base (about 2.5 Ma), comparison between the two records (Fig. 11b) shows that the winter monsoon variation documented in the loess, displays a different pattern from that of the global ice volume changes. Variation in loess-soil grain size is characterised by long-wave cycles superimposed with various higher frequency components, whereas the $\delta^{18}O$ change shows a regular 41 ka oscillation with a rather uniform amplitude (*Raymo et al.,* 1989). From S24 to L32 the loess deposits can be grouped into two different parts - the upper part from S24 to L27 and the lower part, from S27 to L32, each with several closely-spaced soils underlain by a thick loess bed. The two thick loess beds L27 and L32 suggest two lengthy periods with relatively strong winter monsoon and cold climate which are absent in the $\delta^{18}O$ record (*Raymo et al.,* 1989).

In general, correlation of climatic cycles between the grain size and $\delta^{18}O$ records appears not as good as in the younger parts of the record. This may result from both different age estimates for the base of the Olduvai and, in particular, different climatic history. In the site 607 record, orbital tuning yielded an age of about 1.81 Ma for the base of the Olduvai (*Raymo et al.,* 1989), whereas an age similar to the K/Ar-dated record (1.87 Ma) was obtained in the Baoji grain size time scale, thereby suggesting different timing of the climatic events recorded. On the other hand, 41 ka obliquity rhythms for global ice volume variations tend to be dominant over this time interval, as monitored by the DSDP site 607 $\delta^{18}O$ record, whereas orbital components have been detected in the grain size time series. Therefore we speculate that the discordances discussed above may be the result not only of different assumed positions of the Olduvai base in the two time scales, but also, and perhaps largely, from the contrasting regional climatic history.

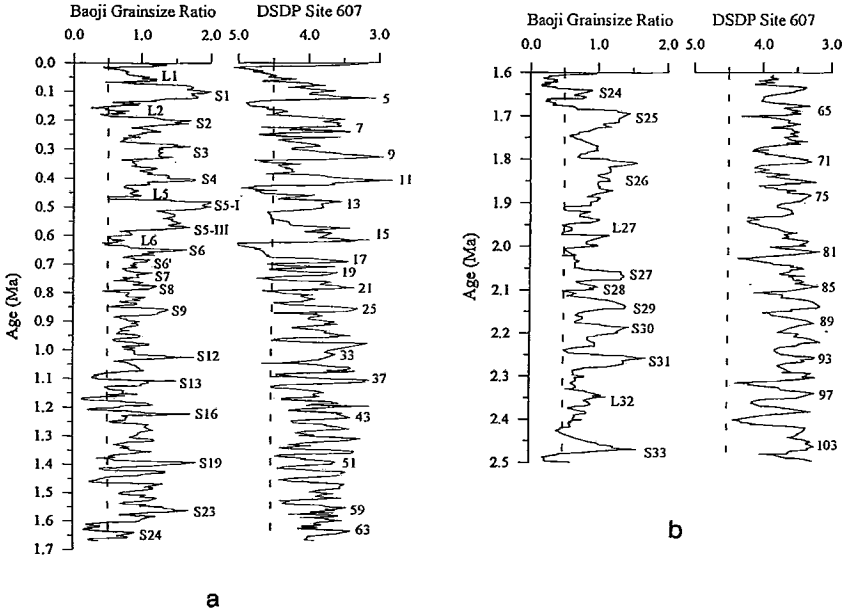

Fig. 11a,b. Comparison of variations in grain size ratio (<2μm/>10μm) of the Baoji section with DSDP site 607 $\delta^{18}O$ record (*Ruddiman et al.*, 1989a). Several soils and loess beds in the Baoji section are labelled S1 and L1 respectively.

In the northwest part of the Loess Plateau we have high resolution grain size and magnetic susceptibility data for the last glacial-interglacial cycle from the Lijia Yuan section (Fig. 3). Here, nearer the loess source, we have relatively thicker deposits of loess deposited within a similar time interval to those found in the southeast. 1233 samples were taken at 2 cm intervals above the base of S1. This sample spacing yields a mean depositional resolution of about 80 years for the last glacial loess L1 and about 200 years for the soil complex S1. This has enabled us to correlate and compare our data with other high resolution climatic proxy records. Figure 12 shows the susceptibility and grain size data from Lijia Yuan, compared to the susceptibility record of Linxia, a section about 150 km southwest of Lijia Yuan. The data are correlative and quite easily differentiates the soil and loess units of the last glacial-interglacial cycle.

Previous studies (*An et al.*, 1991; *Maher et al.*, 1994) suggest that susceptibility variations in the loess-soil sequences are closely related to changes in East-Asia summer monsoon rainfall. Our susceptibility record exhibits one high peak over the Holocene and three high peaks over the last interglacial period, while two complexes of high peaks are seen within L1 (Fig. 12). These peaks, indicating intensified summer monsoon rainfall, correlate well with those in other susceptibility records of the Plateau (*An et al.*, 1991; *Kukla* and *An*, 1989). The susceptibility over other intervals within L1 shows low values and almost a straight line, implying greatly reduced summer monsoon influence during glacial times, probably due to the great distance of Lijia

Yuan to the tropical and subtropical oceans. On the other hand, down-section variations in grain size can be used as an indicator of fluctuations in the intensity of the winter monsoon winds flowing from the Siberia High (*Ding et al.*, 1994). However, because of the proximity of Lijia Yuan to the deserts, changes in loess grain size may have been significantly controlled by the advance-retreat cycles of the deserts.

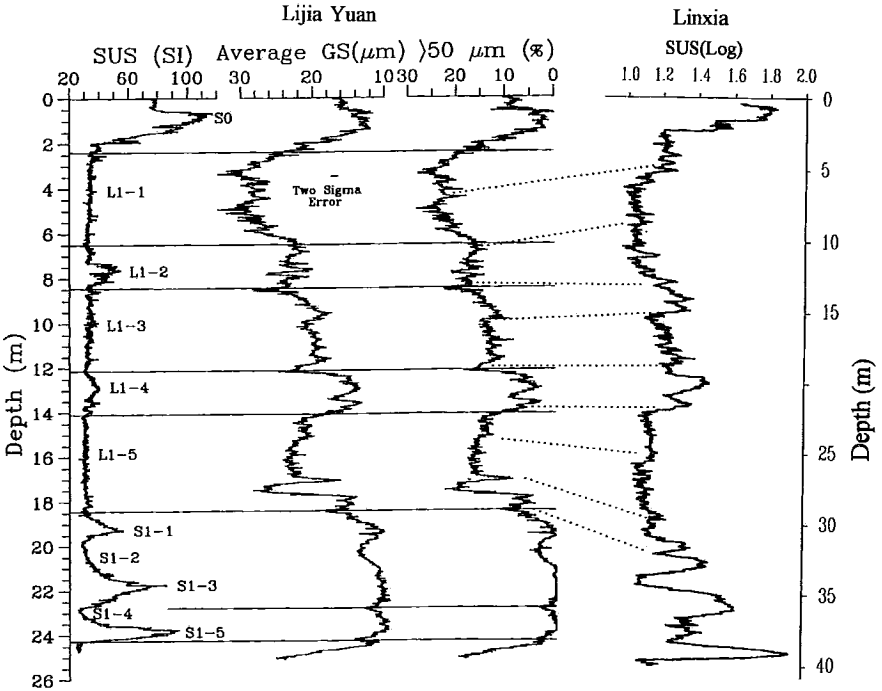

Fig. 12. Magnetic bulk susceptibility and grain size (the average grain size and the percentage of the fraction greater than 50 μm) records in the Lijia Yuan loess section above S1, correlated with the Linxia magnetic susceptibility record (*Chen*, 1995). S0 is the Holocene soil. S1 is the last interglacial soil complex. It consists of three individual soil horizons (S1-1, S1-3, S1-5) and two loess horizons (S1-2, S1-4). L1 is the last glacial loess deposit and can be subdivided into five parts (from L1-1 to L1-5). The boundaries of S0 and S1 are defined in the field, whereas the subdivision of L1 is based on the combined features of the susceptibility and grain size records (see the divide lines). The 2s error bar for the average grain size record is 0.9 μm.

We then compared our data with the isotopic SPECMAP records. As shown in the susceptibility curve (Fig. 13), the three highs and two lows within S1 correlate with the isotope substages 5a to 5e respectively, and the two peaks within L1 with isotope stage 3. The six susceptibility peaks from S0 to S1-5 (Fig. 12) have recorded the influence of the six precessional cycles of the Earth's orbit above the time of about 130 ka ago (*Berger* and *Loutre*, 1991). Based on this correlation, we tuned the susceptibility curve directly to the insolation record at 60° north latitude with a phase lag of 6000 years (*Ding et al.*, 1994; *Imbrie et al.*, 1984; Fig. 13). As climatic variability within L1

is difficult to distinguish in the field, determinations of the boundaries of L1-2 and L1-4 is based on the combined features of the susceptibility and grain size curves (Figs. 12 and 13). Our tuned time scale together with the insolation (*Berger* and *Loutre*, 1991) and SPECMAP (*Imbrie et al.*, 1984) records correlate very well and are tightly constrained over each time interval of about 11,000 years.

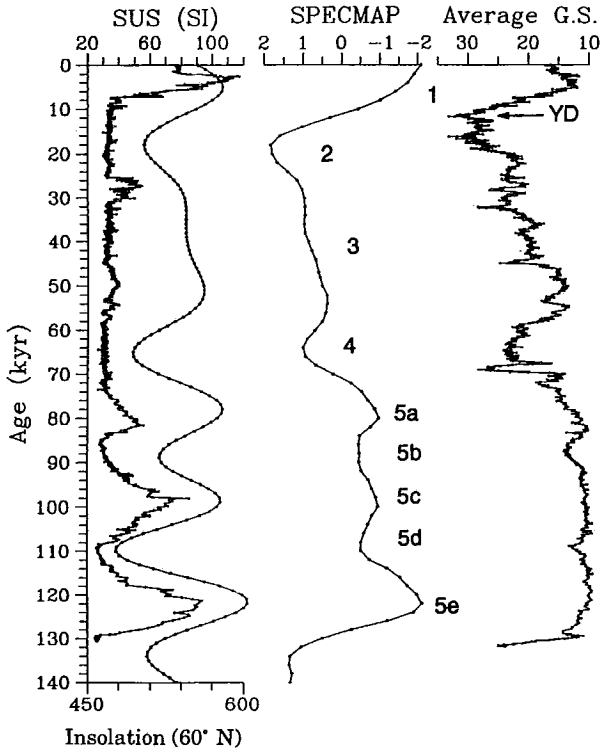

Fig. 13. Comparison of the Lijia Yuan susceptibility and average grain size records with the summer insolation at 60° north latitude, lagged 6000 years (*Berger* and *Loutre*, 1991), and the SPECMAP records (*Imbrie et al.*, 1984). The records are plotted against time scales. The Lijia Yuan loess time scale is derived from tuning the susceptibility curve to the insolation record with a time lag of 6000 years.

When we compare the average grain size record from Lijia Yuan with the GISP2 air temperature record ($\delta^{18}O$) (*Grootes et al.*, 1993) both matches and mismatches are observed (Fig. 14). First, most of the Dansgaard-Oeschger cycles recorded in the Greenland ice cores during the last glacial period have equivalents in the grain size record. The time difference of the climatic events between the two records is within about 1000 years, further corroborating the time scales of both records. This similarity implies that these frequent climatic oscillations could be at least hemispheric. Secondly, *Bender et al.* (1994) have suggested a climate teleconnection between Greenland and

Antarctica by showing the correlation of the longer interstadials 8, 12, 14, 16+17, 19 and 20 between the two areas. In our grain size record, these interstadials (marked with "*" in Fig. 14) are prominently expressed, suggesting a global mechanism in pacing the events. Thirdly, oscillations of the monsoon-desert system display a different pattern with respect to the Greenland $\delta^{18}O$ record. Whereas oscillations in the GISP2 record exhibit a generally uniform amplitude, our record shows that these events are superimposed on a trend toward a gradual increase in winter monsoon intensity and advance of deserts. This trend is consistent with the increase in global glaciation toward the last glacial maximum, as documented in the SPECMAP record (*Imbrie et al.*, 1984; Fig. 13). Fourthly, the grain size data show a greatly enhanced winter monsoon event

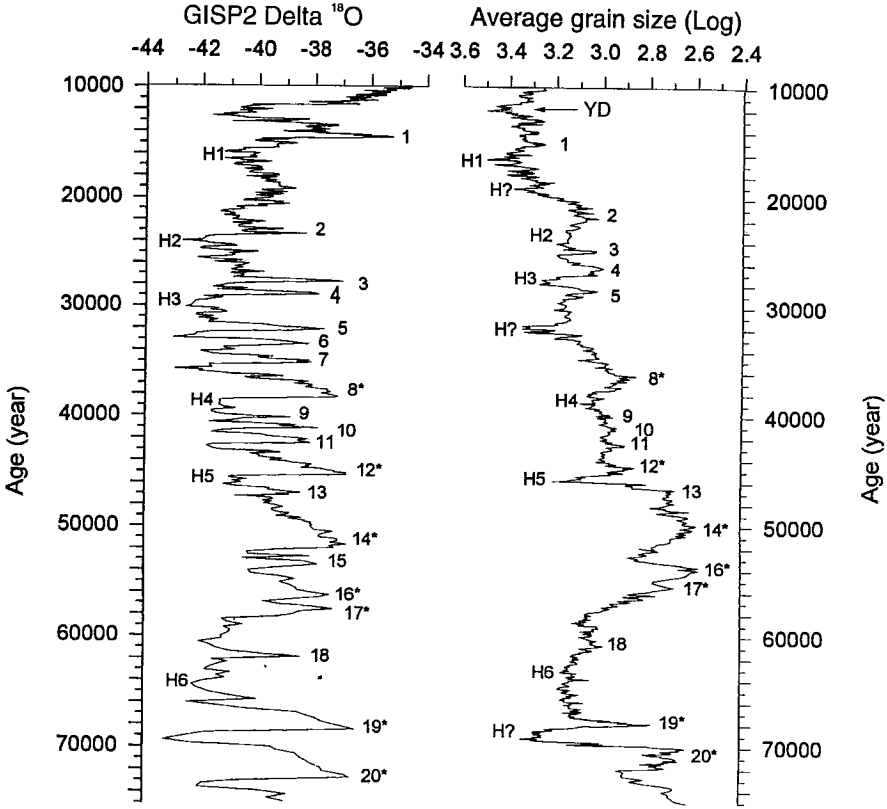

Fig. 14. Correlation between the GISP2 $\delta^{18}O$ (*Grootes et al.*, 1993) and the Lijia Yuan average grain size records in the last glacial period. A correlation is made between the two records for the glacial interstadials (numbered from 1 to 20) identified in the GRIP (*Dansgaard et al.*, 1993) and GISP2 records. The interstadials of longest duration (marked by "*" in both records) are also recognized in Antarctica (*Bender et al.*, 1994). The correlation of the grain size record with the Heinrich events (H1 to H6) is made using *Bond et al.*'s (1993) age designation. The grain size increase events marked with "H?" are not prominently expressed in the ice-rafting records.

around 12,000 yr BP with a time duration of about 1000 years. From this event down to another similar event at about 17,000 yr BP, there are three peaks representing reduced winter monsoon winds, coinciding well with the Greenland record. Therefore, the event that occurred around 12,000 yr BP in our time scale can be confidently interpreted as being coeval of the Younger Dryas in the Greenland record (*Mayewski et al.*, 1993). The grain size record also shows an increase in frequency of climatic oscillations toward the last glacial maximum. In the period of about 15 to 19 ka BP, there are about 9 small grain size cycles, apparently in a time duration less than 500 years. They are not clearly defined in the Greenland record. Fifthly, when we use *Bond et al.*'s (1993) time designation to compare iceberg discharge events in the North Atlantic (Heinrich events) with the grain size record, we found that in the six Heinrich events, only H1, H3 and H5 are accompanied by a rapid increase in winter monsoon intensity and desert advance. Three other significant grain size increase events that occurred at about 19, 32 and 69 ka ago are not prominent in the ice-rafting records. Finally, during the period of the soil S1-5 development, the equivalent of the Eemian interglaciation, our grain size data do not provide any evidence for climatic instability as documented in the GRIP ice core (*Dansgaard et al.*, 1993); and other records (*Field et al.*, 1994; *Thouveny et al.*, 1994). In spite of a Younger Dryas-like event registered in the grain size parameters, near the bottom S1-5 shows a narrow peak (low dust accumulation rate) and fine grain size (Fig. 14), indicating a period of weakened winter monsoon, increased summer monsoon and greatly-retreated deserts. The soil S1-3 (isotope substage 5c) also shows a similar climate condition as S1-5.

6. *Coupled systems*

Comparing our climatic records from north-central China with a variety of proxy records from other areas has enabled us to identify similarities and differences in climatic patterns on a global scale. Why patterns change within or outside a region is, of course, a key question. Although our records show the influence of orbital variations on climate, our understanding of other forcing mechanisms, which may trigger change, is poor. Some explanations, however, are worth exploring.

The abrupt change at about 2.5 Ma when loess deposits began to accumulate in north-central China and the onset of glaciation may have been influenced by the uplift of the Tibetan Plateau. It appears that accelerated uplift of the Tibetan Plateau in the Late Pliocene caused a reorganization of atmospheric circulation in Eastern Asia, favouring deflation, transport and deposition of loess (*Ding et al.*, 1992). The Tibetan Plateau-inland desert-Loess Plateau formed a coupled environmental system and could be key in understanding the initiation of glaciation in the Northern Hemisphere and the evolution of climate in the Quaternary. The uplift triggered a global climatic system in response to orbital forcing, creating a feedback mechanism over eastern Asia at 2.5 Ma and promoting the development of glaciation on a global scale (*Ding et al.*, 1992).

In our analysis of the evolution of the Quaternary climate record from loess sequences, three major climatic shifts have been recorded. The first was at 2.5 Ma, discussed above, the second 1.7 to 1.6 Ma and the third at 0.5 to 0.8 Ma. When we compared our loess data with records from deep sea cores, specifically DSDP 607, we found that cycles and amplitude shifts correlated well except for the records between about 2.5 Ma and 1.6 Ma (*Ding et al.*, 1991; 1994). This suggests that different parts of the climate system could have undergone a coupled and coherent change during the Pleistocene and implies a link may have existed between variations in the East Asian winter monsoon and global ice volume. Previous studies (*Liu et al.*, 1985) demonstrated that loess materials in the Chinese Loess Plateau are transported mainly by the northwesterly monsoon winds away from the Siberian high pressure cells. It is speculated that changes in the Siberian High may be controlled by glacial-age boundary conditions at higher latitudes, particularly by the extent of continental and sea ice cover (*Ding et al.*, 1992). It is thus expected that a coupled change would occur involving winter monsoon intensity and global ice volume. At about 1.7-1.6 Ma BP, the loess grain size variability began to obtain the same climatic periodicities as the marine $\delta^{18}O$ record, that is, 41 ka period. Around the B/M magnetic boundary, a synchronous shift in climate modes occurred in both records. Over this latter period, changes in loess grain size are dominated by a 100-ka climate period, which is characteristic of global ice-sheet variations in the Brunhes chron and thought to originate from a non-linear interaction between orbital precession and obliquity and the ice build-up processes (*Imbrie et al.*, 1993). It is inferred that direct local insolation forcing could be less important in driving the East Asian winter monsoon variability, and alternatively, variations in glacial age boundary conditions may have played a key role in modulating and pacing monsoon strength and timing. The evidence suggests that at about 1.7-1.6 Ma BP the ice-sheets in the Northern Hemisphere may have reached a critical size that was sufficient to influence the East-Asian winter monsoon system, probably through the ice sheets-North Atlantic Deep Water-circum Antarctic surface waters-atmospheric pCO2 mechanism proposed by *Imbrie et al.* (1993). In addition, a direct influence of the ice sheets in the Northern Hemisphere may also be important. Recently, we (*Ding et al.*, 1995) proposed that the enlarged ice sheets in the Northern Hemisphere can result in an increase in land surface albedo over the Siberian region and thermally strengthen the Siberia High. On the other hand, the extended ice sheets can direct more cold polar air to middle latitudes, leading to a significant downstream cooling of the middle latitudes and a dynamic intensification of the Siberia High. Both thermal and dynamic mechanisms may need to be taken into consideration in explaining the coupled variation of the East-Asian winter monsoon with global ice volume changes in the last 1.6 Ma.

What we are puzzled with in this comparison is the regional shift in climate modes at about 1.7-1.6 Ma BP and the strong 400 ka climate period recorded in the loess sequence over the 2.5-1.6 Ma interval. Based on the DSDP site 607 $\delta^{18}O$ record,

Ruddiman et al. (1986) established a dominant 41 ka cycle model for global ice volume oscillations over the Matuyama chron, and this model is further confirmed by other deep-sea cores (*Shackleton et al.*, 1990). However, our winter monsoon record shows a complex periodicity pattern over the lower Matuyama, greatly differing from the $\delta^{18}O$ record (Fig. 11). The discrepancy between loess and deep-sea records implies that during the 2.5-1.6 Ma interval, the influence of global ice volume on other parts of the climate system could be limited because of less ice cover in the Northern Hemisphere. Deep-sea climatic records and benthic $\delta^{18}O$ curves appear to indicate a trend toward increased glaciation since 2.5 Ma BP (*Ruddiman et al.*, 1989a; *Raymo et al.*, 1989; *Shackleton et al.*, 1990). This trend may be related to the tectonic uplift of the Tibetan Plateau, as with the dominant 100-ka periods starting at about 0.8 Ma (*Ruddiman* and *Raymo*, 1988; *Ruddiman* and *Kutzbach*, 1989; *Raymo* and *Ruddiman*, 1992). On the other hand, uplift of the Tibetan Plateau can basically control the position and strength of the Siberia High, as manifested by GCM modelling experiments (*Manabe* and *Terpstra*, 1974; *Kutzbach et al.*, 1989). In this context, it is likely that a critical size of global ice volume and a threshold height of the Tibetan Plateau may be needed to explain the 1.7-1.6 Ma shift in climate regime over East Asia. It should be mentioned, however, that some authors have concluded that the present height of the Tibetan Plateau occurred in the Tertiary (*Coleman* and *Hodges*, 1995).

If the above explanation works, there may be a different mechanism that paced winter monsoon oscillations in the 2.5-1.6 Ma interval compared to later times. In this case, it is convenient to advocate direct local insolation forcing. However, this mechanism will be challenged by the winter monsoon periodicity pattern, i.e. strong 400 ka and weak 23 ka cycles over this time interval. Although changes in the earth orbital eccentricity contain a strong period centered at about 400 ka (*Berger*, 1978), solar insolation variations induced by this orbital parameter are thought to be too small to directly modulate climate changes (*Imbrie et al.*, 1993). Besides, local insolation forcing is supposed to give rise to a strong 23 ka climate period over monsoonal areas, as demonstrated by long proxy records off Africa (*Ruddiman et al.*, 1989b) and in the Indian ocean (*Prell et al.*, 1992). In the loess record, however, this period is weak (Fig. 9). At this stage, the cause of strong 400 ka and week 23 ka climate cycles is unknown and therefore, the problem remains open.

The correlation of our high resolution grain size and susceptibility records showing rapid climate variation with SPECMAP and GISP2 $\delta^{18}O$ records (*Grootes et al.*, 1993) demonstrate that most of the Dansgaard-Oeschger cycles on Polar regions have equivalents on the East-Asian continent. It demonstrates a close relation of the Dansgaard-Oeschger cycles to the monsoon-desert system and the time-dependent evolution of global ice volume. During isotope stage 5, the monsoon-desert system remained "stable" by steadily responding to Earth orbital forcing. When global ice sheets developed towards the maximum stage, oscillations of the system increased greatly. This pattern suggests a linkage between variability in the ice sheets of the

Northern Hemisphere and the Siberian High pressure cell over millennial time scales. Meteorological observations (*Tao* and *Chen*, 1957) demonstrate that cold polar air accumulating in the Siberian region (Fig. 6) flows mostly from the northern Kara Sea (56%) and northwestern Barents Sea (25%). Cold air from the North Atlantic only constitutes 15% of the total. In this respect, oscillations in the strength and position of the Siberian High may have been critically controlled by variations in the ice sheets of the Kara and Barents seas during the last glacial age, together with other sources of forcing. Recent studies (*Fronval et al.*, 1995; *Clark* and *Bartlein*, 1995; *Rahman*, 1995; *Polyak et al.*, 1995) suggest that ice sheets in different parts of the Northern Hemisphere may have undergone coherent fluctuations on millennial time scales. This implies that the Dansgaard-Oeschger cycles cannot be explained solely by the discharge of icebergs into the North Atlantic which can alter the ocean's heat *conveyor (Broecker et al.*, 1992; *Broecker*, 1994). The absence of a good correlation of the Heinrich events with our grain size data that purports a link between the atmosphere and ice volume, further supports this idea. Recently, *Bond* and *Lotti* (1995) suggested a mechanism operating within the atmosphere that caused rapid oscillations in air temperature above Greenland and in calving from more than one ice sheet. Our results appear to reinforce this suggestion.

7. *Summary and conclusions*

The Loess Plateau of north-central China offers one of the most complete Quaternary terrestrial records known. The 37 well-developed paleosols of varying intensity and duration, indicate generally warmer and moister conditions when compared with the loess units that indicate colder and drier periods. The soils give an accurate view of the intensity of summer monsoonal activity and environment whereas the loess beds give an account of the intensity of winter monsoonal activity. Although magnetic susceptiblity have been useful as a climatic proxy, we found that variations in climate at relatively high resolution could be detected by grain size variation within loess units. This led to the development of our grain size time scale based on orbital variations, and independent of any correlation with $\delta^{18}O$ signals in deep-sea sediments. The time scale is tightly constrained and compares favourably with other orbital time scales. In addition, spectral analysis of the grain size record clearly showed time dependent monsoonal periodicities. The same trends were recorded when our grain size time scale was correlated with DSDP 607 site $\delta^{18}O$ records back to 1.67 Ma. The winter monsoon record shows a close correlation with the global ice volume record over this time interval, with the enhanced winter monsoon periods correlating with those of extended ice sheets. Below about 1.67 Ma to 2.5 Ma comparisons between the two records display different patterns, which most likely indicate different climates. We next determined high resolution grain size variations and magnetic susceptibility from the last glacial-interglacial cycle from relatively thick deposits of loess at Lijia Yuan, nearer the loess source. This enabled us to identify the Holocene soil, SO, three soils

within soil S1 representing the last interglacial, and two warm periods in L1. These records correlated well with the isotopic SPECMAP records, and are tightly constrained over each time interval of about 11,000 years. When we compared our average grain size record with the GISP2 (*Grootes et al.*, 1993) air temperature record ($\delta^{18}O$), both matches and mismatches were observed. Among other things, the Dansgaard-Oeschger cycles of the last glacial can be correlated and the Younger Dryas identified. Also, our grain size data does not supply any evidence for climatic instability during the last interglacial as documented by the GRIP (*Dansgaard et al.*, 1993) records.

The wealth of climatic data from the interpretation of the loess-soil sequences in north central China has enabled us to construct climates and environments for the past 2.5 Ma and to identify climate forcing mechanisms. Correlating and comparing our data with other climate proxy records, some from widely-spaced geographical areas, has provided the information necessary to couple climatic systems and to make inferences as both regional and global climatic patterns. These include the influence of the uplift of the Tibetan Plateau on the worldwide change of climate at about 2.5 Ma, a link between the variations in the East Asian winter monsoon and global ice volume, and that our high resolution climatic records can be compared to other high resolution records identifying regional and perhaps global, rapid, short term (millennial scale) climatic oscillations.

Acknowledgements

The Baoji grain size analyses were performed in the Xian Laboratory of Loess and Quaternary Geology, Academia Sinica. We thank Prof. Z.S. An for his arrangement of the laboratory work. We also acknowledge Jianzhang Ren and Jimin Sun for grain size analyses of the Lijia Yuan samples. This study was supported by the National Natural Science Foundation of China, the Chinese Academy of Sciences, and the Natural Sciences and Engineering Council of Canada (NSERC).

8. *References*

An, Z.S., G. Kukla, S.C. Porter and J.L. Xiao, 1991. Magnetic susceptibility evidence of monsoon variation on the loess plateau of central China during the last 130,000 years. *Quaternary Research,* **36,** 29-36.

Baksi, A.K., V. Hsu, M.O. McWilliams and E. Farrar, 1992. $^{40}Ar/^{39}Ar$ dating of the Brunhes-Matuyama geomagnetic reversal. *Science* **256**, 356-357.

Bender, M., T. Swoers, M.L. Dickson, J. Orchardo, P. Grootes, P.A. Mayewski and D.A. Meese, 1994. Climate correlations between Greenland and Antarctica during the past 100,000 years. *Nature,* **372**, 663-666.

Berger, A., 1978. Long-term variations of caloric insolation resulting from the Earth's orbital elements. *Quaternary Research*, **9**, 139-167.

Berger, A. and M.F. Loutre, 1991. Insolation values for the climate of the last 10 million years. *Quaternary Science Reviews,* **10**, 297-317.

Bond, G., W. Broecker, S. Johnsen, J. McManus, L. Labeyrie, J. Jouzel and G. Bonani, 1993. Correlations between climate records from North Atlantic sediments and Greenland ice. *Nature*, **365**, 143-147.

Bond, G.C. and R. Lotti, 1995. Iceberg discharges into the North Atlantic on millennial time scales during the last glaciation. *Science,* **267**, 1005-1010.

Broecker, W.S., G. Bond, M. Klas, E. Clark and J. McManus, 1992. Origin of the northern Atlantic's Heinrich events. *Climate Dynamics* **6**, 265-273.

Broecker, W.S., 1994. Massive iceberg discharges as triggers for global climate change. *Nature*, **372,** 421-424.

Chen, F.H., 1995. Uplift of Qinghai-Xizang (Tibet) plateau and global change. Ed. Li Jijun, Lanzhou University Press, 130-180.

Clark, P.U. and P.J. Bartlein, 1995. Correlation of late Pleisocene glaciation in the western United States with North Atlantic Heinrich events. *Geology,* **23,** 483-486.

Coleman, M. and K. Hodges, 1995. Evidence for Tibetan Plateau uplift before 14 myr ago from a new minimum age for east-west extension. *Nature*, **374,** 49-52.

Dansgaard, W., S.J. Johnsen, H.B. Clausen, D. Dahl-Jensen, N.S. Gundestrup, C.U. Hammer, C.S. Hvidberg, J.P. Steffensen, A.E. Sveinbjörnsdottir, J. Jouzel and G. Bond, 1993. Evidence for general instability of past climate from a 250-kyr ice-core record. *Nature*, **364,** 218-220.

Ding, Z.L., J.T. Han, C. Liu and T.S. Liu, 1991. Preliminary determination of an abrupt climatic shift in North China at about 2.5 Ma. *Chinese Science Bulletin,* **36**, 852-856.

Ding, Z.L., N. Rutter, J.T. Han and T.S. Liu, 1992. A coupled environmental system formed at about 2.5 Ma over eastern Asia. *Palaeogeography, Palaeoclimatology, Palaeoecology*, **94**, 223-242.

Ding, Z.L., N.W. Rutter and T.S. Liu, 1993. Pedostratigraphy of Chinese loess deposits and climatic cycles in the last 2.5 Ma. *Catena,* **20**, 73-91.

Ding, Z., Z. Yu, N.W. Rutter and T. Liu, 1994. Towards an orbital time scale for Chinese loess deposits. *Quaternary Science Reviews*, **13**, 39-70.

Ding, Z., T. Liu, N. Rutter, Z. Yu, Z. Guo and R. Zhu, 1995. Ice volume forcing of East Asian winter monsoon in the past 800,000 years. *Quaternary Research*, **44**, 149-159.

Field, M.H., B. Huntley and H. Müller, 1994. Eemian climate fluctuations observed in a European pollen record. *Nature*, **371,** 779-783.

Fronval, T., E. Jansen, J. Bloemendal and S. Johnsen, 1995. Oceanic evidence for coherent fluctuations in Fennoscandian and Laurentide ice sheets on millennium timescales. *Nature*, **347,** 443-446.

Grootes, P.M., M. Stuiver, J.W.C. White, S. Johnsen and J. Jouzel, 1993. Comparison of oxygen isotope records from the GISP2 and GRIP Greenland ice cores. *Nature*, **366**, 552-554.

Heller, F. and T.S. Liu, 1984. Magnetism of Chinese loess deposits. *Geophysical Journal*, Royal Astronomical Society, **77**, 125-141.

Imbrie, J. and J.Z. Imbrie, 1980. Modeling the climatic response to orbital variations. *Science*, **207**, 943-953.

Imbrie, J., J.D. Hays, D.B. Martinson, A. McIntyre, A.C. Mix, J.J. Morley, N.G. Pisias, W.L. Prell and N.J. Shackleton, 1984. The orbital theory of Pleistocene climate: Support from a revised chronology of the marine delta ^{18}O record. *In:* Berger, A., J. Imbrie, J. Hays, G. Kukla and B. Saltzman, (Eds), *Milankovitch and Climate, Part I*, 269-305. D. Reidel Publishing Co., Dordrecht, Netherlands.

Imbrie, J., A. Berger, E.A. Boyle, S.C. Clemens, A. Duffy, W.R. Howard, G. Kukla, J. Kutzbach, D.G. Martinson, A. McIntyre, A.C. Mix, B. Molfino, J.J. Morley, L.C. Peterson, N.G. Pisias, W.L. Prell, M.E. Raymo, N.J. Shackleton and J.R. Toggweiler, 1993. On the structure and origin of major glaciation cycles. 2. The 100,000-year cycle. *Paleoceanography* **8**, 699-735.

Kukla, G., 1987. Loess stratigraphy in central China. *Quaternary Science Reviews* **6**, 191-219.

Kukla, G., F. Heller, X.M. Liu, T.C. Xu, T.S. Liu and Z.S. An, 1988. Pleistocene climates in China dated by magnetic susceptibility. *Geology,* **16**, 811-814.

Kukla, G. and Z.S. An, 1989. Loess stratigraphy in central China. *Palaeogeography, Palaeo-climotology, Palaeoecology*, **72,** 203-225.

Kutzbach, J.E., P.J. Guetter, W.F. Ruddiman and W.L. Prell, 1989. Sensitivity of climate to late Cenozoic uplift in southern Asia and the American west: Numeral experiments. *Journal of Geophysical Research,* **94,** 18393-18407.

Liu, T.S. et al. (unnamed), 1966. Composition and Texture of Loess. Science Press, Beijing. [in Chinese]

Liu, T.S. et al. (unnamed), 1985. Loess and the Environment. Science Press, Beijing.

Liu, X.M., J. Shaw, T.S. Liu, F. Heller and B.Y. Yuan, 1992. Magnetic minerology of Chinese loess and its significance. *Geophysical Journal International,* **108,** 301-308.

Maher, B.A. and R. Thompson, 1991. Mineral magnetic record of the Chinese loess and paleosols. *Geology,* **19,** 3-6.

Maher, B.A., R. Thompson and L.P. Zhou, 1994. Spatial and temporal reconstructions of changes in Asian paleomonsoon: A new mineral magnetic approach. *Earth and Planetary Science Letters*, **125,** 462-471.

Manabe, S. and T.B. Terpstra, 1974. The effects of mountains on the general circulation of the atmosphere as identified by numeral experiments. *Journal of the Atmospheric Sciences*, **31,** 3-42.

Mayewski, P.A., L.D. Meeker, S. Whitlow, M.S. Twickler, M.C. Morrison, R.B. Alley, P. Bloomfield and K. Taylor, 1993. The atmosphere during the Younger Dryas. *Science,* **261,** 195-197.

Polyak, L., S.L. Lehman, V. Gataullin and A.J.T. Jull, 1995. Two-step deglaciation of the southeastern Barents Sea. *Geology*, **23**, 567-571.

Prell, W., D.W. Murray, S.C. Clemens and D.M. Anderson, 1992. Evolution and variability of the Indian ocean summer monsoon: Evidence from the western Arabian Sea drilling program. *Geophysical Monograph*, **70**, 447-469.

Rahman, A., 1995. Reworked nannofossils in the North Atlantic Ocean and subpolar basins: Implications for Heinrich events and ocean circulation. *Geology*, **23**, 487-490.

Raymo, M.E., W.F. Ruddiman, J. Backman, B.M. Clement and D.G. Martinson, 1989. Late Pliocene variations in northern hemisphere ice sheet and North Atlantic Deep Water circulation. *Paleoceanography,* **4**, 413-446.

Raymo, M.E. and W.F. Ruddiman, 1992. Tectonic forcing of late Cenozoic climate. *Nature*, **359,** 117-122.

Ruddiman, W.F., M.E. Raymo and A. McIntyre, 1986. Matuyama 41,000-year cycles: North Atlantic ocean and northern hemisphere ice sheets. *Earth and Planetary Science Letters*, **80**, 117-129.

Ruddiman, W.F. and M.E. Raymo, 1988. Northern hemisphere climate regimes during the past 3 Ma: Possible tectonic connections. *Philosophical Transactions of the Royal Society of London,* **B318,** 411-430.

Ruddiman, W.F. and J.E. Kutzbach, 1989. Forcing of late Cenozoic northern hemisphere climate by plateau uplift in southern Asia and American West. *Journal of Geophysics Research,* **94,** 18409-18427.

Ruddiman, W.F., M.E. Raymo, D.G. Martinson, B.M. Clement and J. Backman, 1989a. Pleistocene evolution: Northern hemisphere ice sheets and North Atlantic ocean. *Paleoceanography,* **4,** 353-412.

Ruddiman, W.F., M. Sarnthein, J. Backman, J.G. Baldauf, W. Curry, L.M. Dupont, T. Janecek, E.M. Pokras, M.E. Raymo, B. Stabell, R. Stein and R. Tiedemann, 1989b. Late Miocene to Pleistocene evolution of climate in Africa and the low-latitude Atlantic. *Overview of Leg 108 results. Preceedings of the Ocean Drilling Program, Scientific Results*, **108,** 463-484.

Rutter, N.W., Z.L. Ding, M.E. Evans and Y.C. Wang, 1990. Magnetostratigraphy of the Baoji loess-paleosol section in the north-central China Loess Plateau. *Quaternary International,* **7-8**, 97-102.

Rutter, N.W., Ding, Z.L., Evans, M.E. and Liu, T.S., 1991. Baoji-type pedostratigraphic section, Loess Plateau, north-central China, *Quaternary Science Reviews,* **10**, 1-22.

Rutter, N., 1992. Presidential Address, XIII INQUA Congress 1991. Chinese loess and global change. *Quaternary Science Reviews,* **11,** 275-281.

Rutter, N.W. and Z. Ding, 1993. Paleoclimates and monsoon variations interpreted from micromorphogenic features of the Baoji paleosols, China. *Quaternary Science Reviews,* **12,** 853-862.

Rutter, N.W., J. Chlachula and M.E. Evans, 1995. Magnetic susceptibility and remanence record of the Kurtak Loess, Southern Siberia, Russia. *In:* INQUA XIV Congress Abstract Volume, Freie Universitat, Berlin, 235.

Shackleton, N.J., A. Berger and W.R. Peltier, 1990. An alternative astronomical calibration of the lower Pleistocene time scale based on ODP site 677. *Philosophical Transactions of the Royal Society,* Edinburgh **81**, 251-261.

Tao, S.Y. and L.X. Chen, 1957. The atmospheric structure over Asian continent in summer. *Bulletin of Meteorology*, **28**, 234-246. [in Chinese]

Tauxe, L., A.D. Deino, A.K. Behrensmeyer and R. Potts, 1992. Pinning down the Brunhes/Matuyama and upper Jaramillo boundaries: A reconciliation of orbital and isotopic time scales. *Earth and Planetary Science Letters*, **109**, 561-572.

Thouveny, N., J.L. de Beaulieu, E. Bonifan, K.M. Creer, J. Guiot, M. Icole, S. Johnsen, J. Jouzel, M. Reille, T. Williams and D. Williamson, 1994. Climate variations in Europe over the past 140 kyr deduced from rock magnetism. *Nature*, **371,** 503-506.

Williams, D.F., R.C. Thunell, E. Tappa, D. Rio and I. Raffi, 1988. Chronology of the Pleistocene oxygen isotope record: 0-1.88 m.y. BP. *Paleogeography, Paleoclimatology, Paleoecology*, **64**, 221-240.